JOURNAL OF MATERIALS SCIENCE 28 (1993) 5592–5602

Mechanistically based fatigue-damage evolution model for brittle matrix fibre-reinforced composites

V. RAMAKRISHNAN, N. JAYARAMAN
Department of Materials Science and Engineering, University of Cincinnati, Cincinnati, OH 45221, USA

An analysis of the fatigue-damage evolution process through prediction of stiffness drop in brittle matrix unidirectional composites reinforced with continuous stiff fibres is presented. The drop in stiffness of the composite is calculated by partitioning the total damage between the components of the composite, namely the matrix, the fibre, and the interface. Predictions of drop in stiffness are validated for different fatigue test conditions in borosilicate glass-ceramic matrix–Nicalon fibre-reinforced composites. In addition, fatigue test results from other composite systems, such as LASII–Nicalon and aluminosilicate–Nicalon, are examined in the light of this model.

1. Introduction

Ceramic and glass-ceramic matrices reinforced with stiff continuous fibres are being developed for several demanding applications [1, 2]. It is essential to understand and predict the damage development in these materials for their efficient use in any structural application. It has generally been identified in brittle matrix (polymer, ceramic, glass-ceramic) composites, that the stiffness of the composite decreases with increasing fatigue damage [3–8]. The mechanisms of initiation and development of damage leading to final failure of the composite have been well documented [9].

There are several damage development models which associate specific damage mechanisms with specific periods in the life of the composite [10, 11]. These models are generally qualitative in nature. At the other end of the spectrum, there exist models which are mathematically rigorous but practically difficult to verify [12]. Some damage models are associated only with specific failure mechanisms, e.g. delamination [13] or transverse cracking [14]. There are many models which propose equations for predicting damage but are empirical in nature [15–20].

In this paper, a mechanistically based fatigue-damage prediction model for unidirectional fibre-reinforced brittle matrix composites is presented. This model predicts the drop in composite stiffness as a function of time (or number of fatigue cycles) for a known set of fatigue conditions, using mechanical properties of the constituents. The model is validated using experimental results from Nicalon fibre-reinforced borosilicate glass-ceramic matrix composites [21, 22]. In addition, fatigue test results from other composite systems, such as LASII–Nicalon [7] and aluminosilicate–Nicalon [6] are examined in the light of this model.

2. Development of the fatigue-damage model

The mechanical behaviour of a composite as a whole depends upon the response of its constituents, namely the fibre, the matrix and the interface. Thus, any physically based damage model must use contributions from individual constituents as building blocks to determine the overall damage to the composite. It is generally known that the fatigue damage in brittle matrix composites consists of a sequence of events starting from matrix cracking, crack bridging, fibre/matrix debonding, fibre breakage, leading to final failure. This physical description of the damage evolution process is schematically shown in Fig. 1. The presence or absence of any of the damage events depends on a number of material factors, such as the relative mechanical, and thermal properties of the fibre and matrix and the strength of the fibre/matrix bonding.

For a continuous fibre-reinforced composite, the longitudinal rule of mixtures stiffness is

$$E_c = E_m V_m + E_f V_f \quad (1a)$$

or

$$1 = E_m V_m / E_c + E_f V_f / E_c \quad (1b)$$

where E_c, E_m and E_p are the stiffness of the composite, matrix and fibre, respectively, V_m and V_f are the volume fractions of the matrix and fibre, respectively.

The degradation of each constituent occurs at a uniform rate which is determined by the fatigue loading conditions, i.e. stress level, temperature, etc. To predict the stiffness, E, at any given time during the fatigue-damage process, Equation 1a can now be modified to give

$$E/E_c = 1 - E_m V_m / E_c^* \text{ (rate factor 1)} \quad (2a)$$

0022–2461

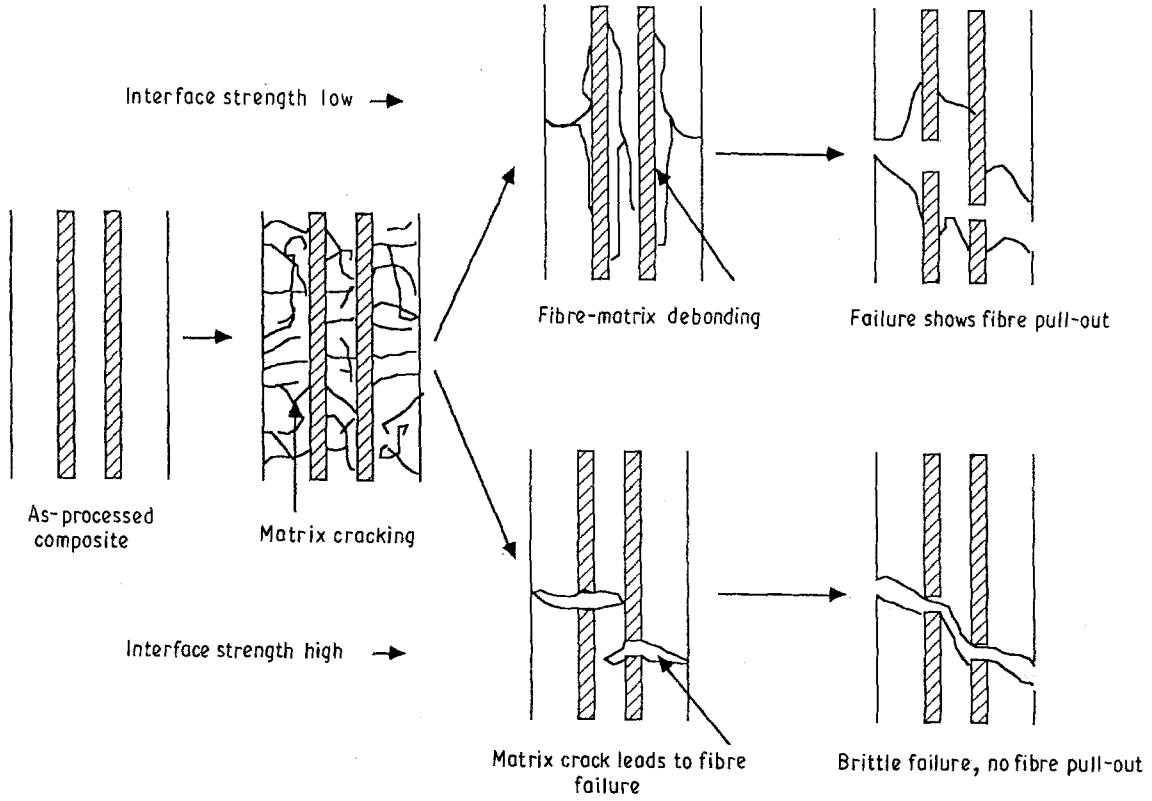

Figure 1 Schematic depiction of the progression of fatigue damage under different interfacial conditions.

$$= -E_f V_f / E_c^* \text{ (rate factor 2)} \quad (2b)$$

In this model, a combination of logarithmic and linear decay functions of time (or cycles) was associated with the stiffness drops for the different damage processes. (The exact mechanistic reasons for the logarithmic/linear decay functions are not clear now. Additional work is in progress in several composite systems to identify these reasons.) The total stiffness drop as a function of the number fatigue cycles is described by a general equation of the form

$$E/E_c = 1 - A^*[\{(1 - f)^* \ln(N + 1)\} + f^* N] - B^* \ln(1 - N/N_f) \quad (3a)$$

where A, B and f are constants that will be shown to be related to composite constituent properties and N_f is the number of cycles to failure at the given applied fatigue stress. Again, it has been demonstrated that applied fatigue stress versus N_f follows a power law life equation of the type $\sigma_{app} = \sigma^*_{uts}(2N_f)^b$, where $2N_f$ is the number of reversals (1 cycle = 2 reversals) to failure, σ_{uts} is the fatigue strength coefficient (= monotonic tensile strength), and b is the fatigue strength exponent. This relationship has been demonstrated for glass fibre-reinforced epoxy systems [15] and for Nicalon fibre-reinforced borosilicate glass-ceramic system [22].

2.1. Specific case ($f = 0$) – poor fibre/matrix interface strength

The factor f in Equation 3a was found to represent the fibre/matrix interface shear strength and can take values from 0–1. In the specific case of $f = 0$ (corresponding very little interface strength), the equation simplifies to

$$E/E_c = 1 - A^* \ln(N + 1) - B^* \ln(1 - N/N_f) \quad (3b)$$

for $N = 0$ to $N = N_f - 1$, where, N is the number of cycles in the damage process, and N_f the number of cycles to failure. At $N = N_f - 1$

$$E/E_c = 1 - \{A^* \ln(N_f)\} - B^* \ln(1/N_f) \quad (4)$$

Examination of Equation 4 indicates that the stiffness of the composite just prior to failure is obtained by subtracting two terms from the initial stiffness ($E/E_c = 1$). Intuitively, one might suspect that one of these terms might be due to the matrix and the other due to the fibre. As we assume at a time just prior to final failure that the matrix is entirely degraded and the fibres are degraded up to a point where the composite can no longer withstand the applied load, we can further conclude from Equation 4 that

$$A^* \ln(N_f) = E_m V_m / E_c \quad (5)$$

(the entire stiffness reduction due to degradation of the matrix just before final failure), and that

$$B^* \ln(1/N_f) = E_f V_f / E_c^*(1 - r) \quad (6)$$

(the entire stiffness reduction from the broken fibres just before final failure), where $(1 - r)$ represents the fraction of remaining net cross-section at the time of failure. This is applied only to the damage term for fibres because the matrix cracking occurs early in the fatigue process when the overall composite is intact, while during the fibre breakage process, the effect due to the reduction of cross-section and the load-carrying

capability of the composite is significantly affected. This fraction of the net cross-section of the composite at the time of failure can be calculated. If the ultimate tensile strength of the composite is denoted σ_{uts} and the applied tensile fatigue stress and load denoted by σ_{appl} and P_{appl}, respectively, and A_o and A_{fail} are the original and final cross-sectional area of the composite, then it can be said that $P_{appl}/A_o = \sigma_{appl}$, and $P_{appl}/A_{fail} = \sigma_{uts}$, or $\sigma_{appl}/\sigma_{uts} = A_{fail}/A_o = r$.

Equations 5 and 6 predict the stiffness drops due to each of the damage processes. The damage evolution equation can then be written as

$$E/E_c = 1 - E_m V_m/E_c^*\{\ln(N + 1)/\ln(N_f)\} + E_f V_f/E_c^*(1 - r)^*\{\ln(1 - N/N_f)/\ln(1/N_f)\} \quad (7)$$

2.2. General case ($0 < f < 1$) – varying fibre/matrix interface strength

Now let us consider the general case of composite systems with strong fibre/matrix interfaces. Equation 3a can be rewritten by substituting for A and B from Equations 5 and 6 to give

$$E/E_c = 1 - E_m V_m/E_c^*[(1 - f)^*\{\ln(N + 1)/\ln(N_f)\} + f^*(N/N_f)] + E_f V_f/E_c^*(1 - r)^* \{\ln(1 - N/N_f)/\ln(1/N_f)\} \quad (8)$$

Here, the stiffness reduction due to matrix damage appears to be partitioned between the two rate processes, one logarithmic, the other linear. The partitioning is done through a fibre/matrix interface strength parameter, f. The interface is the least understood but the most influencial factor in the determination of composite properties. As we will see later when applying this model to experimental results in glass-ceramic matrix composites, f is the friction coefficient as determined by the fibre push-out test [23].

Equations 7 and 8 thus represent the mechanistically based damage equations that can be used for predicting stiffness drops as a function of cycles in a unidirectional brittle matrix fibre-reinforced composites for two cases, one a general case with variable fibre/matrix interface strength and another a specific case where the interface region is very weak, leading to the physical damage model shown in Fig. 1.

All the parameters used in these equations are mechanical properties of the constituents used in the composite. We will now validate this model with results from several test conditions in the borosilicate glass-ceramic matrix–Nicalon fibre composite system.

3. Application of the model

3.1. Application to the borosilicate glass-ceramic matrix–Nicalon fibre composite system

The fatigue test conditions, and results for the unidirectional borosilicate glass ceramic matrix–Nicalon fibre composites are summarized in Table I. Load-controlled axial fatigue experiments were conducted at room temperature and at 540 °C. Composites containing different volume fractions of the fibres were considered for analyses. The fatigue life power law equation between σ_{appl} and N_f was determined for the different test temperatures and volume fractions and the constants are also listed in this Table II. A detailed discussion of these results, together with the microstructural damage evolution mechanisms are described in [22].

In all the experiments the stiffness of the composite was monitored. In the borosilicate–Nicalon composite system, the stiffness was monitored by measuring strain by both a MTS-type high-temperature extensometer and by the actuator stroke displacement (using an LVDT). While the extensometer gave the strain due to displacement in the gauge length of the specimen, the LVDT gave the strain due to total displacement of the specimen. In addition, the strain measured by the extensometer was shown to be very sensitive to local damage events leading to sudden drops or gradual "hardening", while the LVDT measurements were more global representative of the whole specimen. For this reason, here the stiffnesses measured from the LVDT displacements were used. A more detailed discussion of this observation is given in [22].

TABLE I Summary of fatigue test results [22]

Specimen/batch	V_f[a]	$E_{c,init}$[b] (GPa)	Temp. (°C)	Stress level (MPa)	N_f
4A[c]/A	0.55	109	540	210	150 000
4B/A	0.51	99	540	412	277
4C/A	0.60	117	540	305	1 900
20–3[c]/B	0.50	109	540	160	100 000
32–5/B	0.35	80.5	540	180	3 982
20–2[d]/B	0.50	—	540	180	4 350
20–5/B	0.50	122.5	540	200	302
32–4/B	0.35	85.5	540	200	316
42–1/B	0.42	93	540	200	265
34–6/B	0.30	86	RT	180	95
34–8/B	0.24	77	RT	160	31 276

Note: The plates made from Batch A exhibited higher strength for similar volume fractions of fibres compared to Batch B. It is believed that while the strength is affected due to microstructural differences (such as amount and distribution of α-cristobalite in the matrix) between the two batch of samples, the initial stiffness ($E_{c,init}$) is not significantly affected.

[a] Actual volume fraction of fibres in the tested specimen, measured by quantitative metallography techniques.

[b] The stiffness measured in the first cycle.

[c] No stiffness drop observed.

[d] Stiffness data not recorded. Life data used for power law correlation.

TABLE II Constants from power law correlation

Temperature (°C)	V_f	σ_{uts} (MPa)[a]	b
540	0.50–0.60	500	– 0.0705
540	0.35–0.50	250	– 0.0388
RT	0.25–0.30	200	– 0.0205

[a] From the power law stress life equation. At 540 °C, the actual σ(uts) determined through monotonic tensile tests differed slightly from these values, which was attributed to strain rate differences between the tensile and fatigue tests [21, 22].

The starting stiffness of the composite, E_c, was determined from the first cycle data. In general, the starting stiffness was less than the stiffness predicted by the ideal rule of mixtures analysis. This deviation from the rule of mixtures could be due to a number of reasons, including prior matrix cracking, imperfect fibre/matrix bonding, etc. Here, the difference between the ideal rule of mixture starting stiffness and the actual stiffness has been accounted for by reduced matrix contribution to the total stiffness, i.e. all fibres contributed to the total starting stiffness. Based on this assumption, the ratios $E_f V_f/E_c$ and $E_m V_m/E_c$ (modified) $= 1 - E_f V_f/E_c$ were computed. For test conditions at 540 °C, the σ_{appl} and σ_{uts} are known. At this temperature, the fibre–matrix bond was considered to be very weak, resulting in considerable fibre pull-out, and therefore, the factor, f, was assumed to be 0. A room temperature, the exact bond strength for this composite system is not known. However, Bright *et al.* [24] have determined for a SiC (AVCO SCS6 monofilament of about 140 μm diameter)–borosilicate glass system the friction coefficient (τ/σ_{resid}) to be 0.3

TABLE III Values used for predictions on borosilicate–Nicalon system

Specimen	$\frac{E_m V_m}{E_c}$	$\frac{E_f V_f}{E_c}$	$1 - \{\sigma_{app}/\sigma_{uts}\}$	f	N_f
4A	—	—	—	—	150000
4B	0.021	0.979	0.18	0	277
4C	0.026	0.974	0.39	0	1900
20–3[b]	—	—	—	—	100000
32–5	0.174	0.826	0.28	0	3982
20–2[c]	—	—	—	—	4350
20–5	0.224	0.776	0.20	0	302
32–4	0.221	0.779	0.20	0	316
42–1	0.142	0.858	0.20	0	265
34–6	0.334	0.666	0.10	0.6	95
34–8	0.412	0.588	0.20	0.6	31276

[a] $E_m V_m/E_c$ (modified) $= 1 - (E_f V_f/E_c)$.
[b] No drop in stiffness.
[c] Stiffness data not recorded. Life data used for power law correlation.

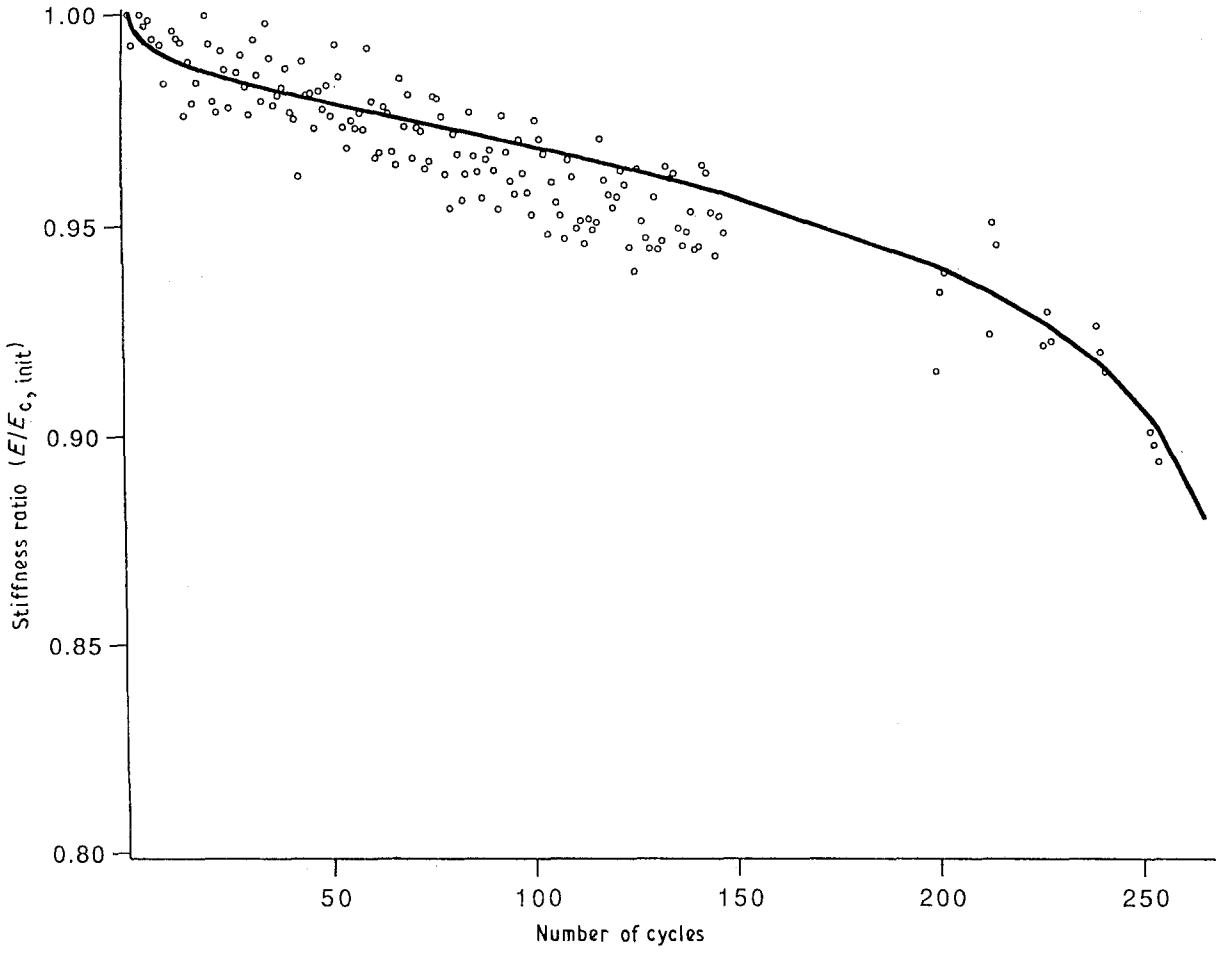

Figure 2 The predicted stiffness curve (—) for specimen 4B (Table I) with the experimental data (○) superimposed.

through a fibre push-out experiment. Nicalon fibres used in this research were about 10–15 μm diameter and the exact friction coefficient for this system is not known. In the present analysis, a value of 0.6 fitted the data very well. Table III lists the parameters such as $E_f V_f/E_c$, $E_m V_m/E_c$ (modified), σ_{uts}, σ_{appl}, f, and N_f for each of the test conditions.

The damage-evolution model was applied to a number of test conditions shown in Table I. The correlation between the predicted and actual observed drop in stiffness in all cases was excellent. Figs 2–8 show typical examples of such correlation.

3.2. Application to other glass-ceramic composite systems

Prewo [7] has reported results from flexural fatigue tests on unidirectional lithium aluminosilicate (LAS) matrix–Nicalon fibre composites. The stiffness of the composite was found to decrease with increasing cycling if the applied cyclic stress was higher than the "proportional limit" (stress below which linear stress–strain behaviour is observed) of the composite.

The stiffness was found to decrease gradually with cycling in the earlier portion of the life, whereas a rapid reduction in stiffness was observed in the last 10% or so of the life of the specimen. We will generate a predicted stiffness drop curve using the data provided, i.e. $E_c = 118\,\text{GPa}$, $E_f = 190\,\text{GPa}$, $V_f = 0.45 - 0.5$, $\sigma_{uts} = 1000 - 1100\,\text{MPa}$, $\sigma_{appl} = 374\,\text{MPa}$, $N_f = 250$ cycles. The starting stiffness is less than that predicted by the rule of mixtures, which indicates imperfect bonding between the fibre and matrix. This has been previously reported by Brennan [25], Cooper and Chyung [26] and Bischoff *et al.* [27] for LAS–Nicalon composites due to the formation of a carbon layer at the interface. Using the procedure described above, $E_m V_m/E_c$ (modified) and $E_f V_f/E_c$ are calculated to be 0.195 and 0.805, respectively.

In the absence of information on the fibre/matrix interface, the stiffness drop was calculated using Equation 8 for various values of f and the predicted stiffness versus number of cycles is plotted in Fig. 9. Increasing f tends to make the rate of stiffness drop to be uniformly high through most of the life of the composite, whereas decreasing f tends to encourage the presence of two stages, i.e. an initial rapid drop stage followed by a slower, steady drop in stiffness. According to this figure, fibre failure is predicted to start at about 225 cycles for all f values. In the absence of quantitative data, this prediction seems to agree well with the qualitative observations of Prewo [7], wherein he states "Specimen failure was taken to occur at the 200th cycle in that the specimen indicated a marked decrease in stiffness. The load–deflection traces between cycles 225 and 250 indicate that the specimen

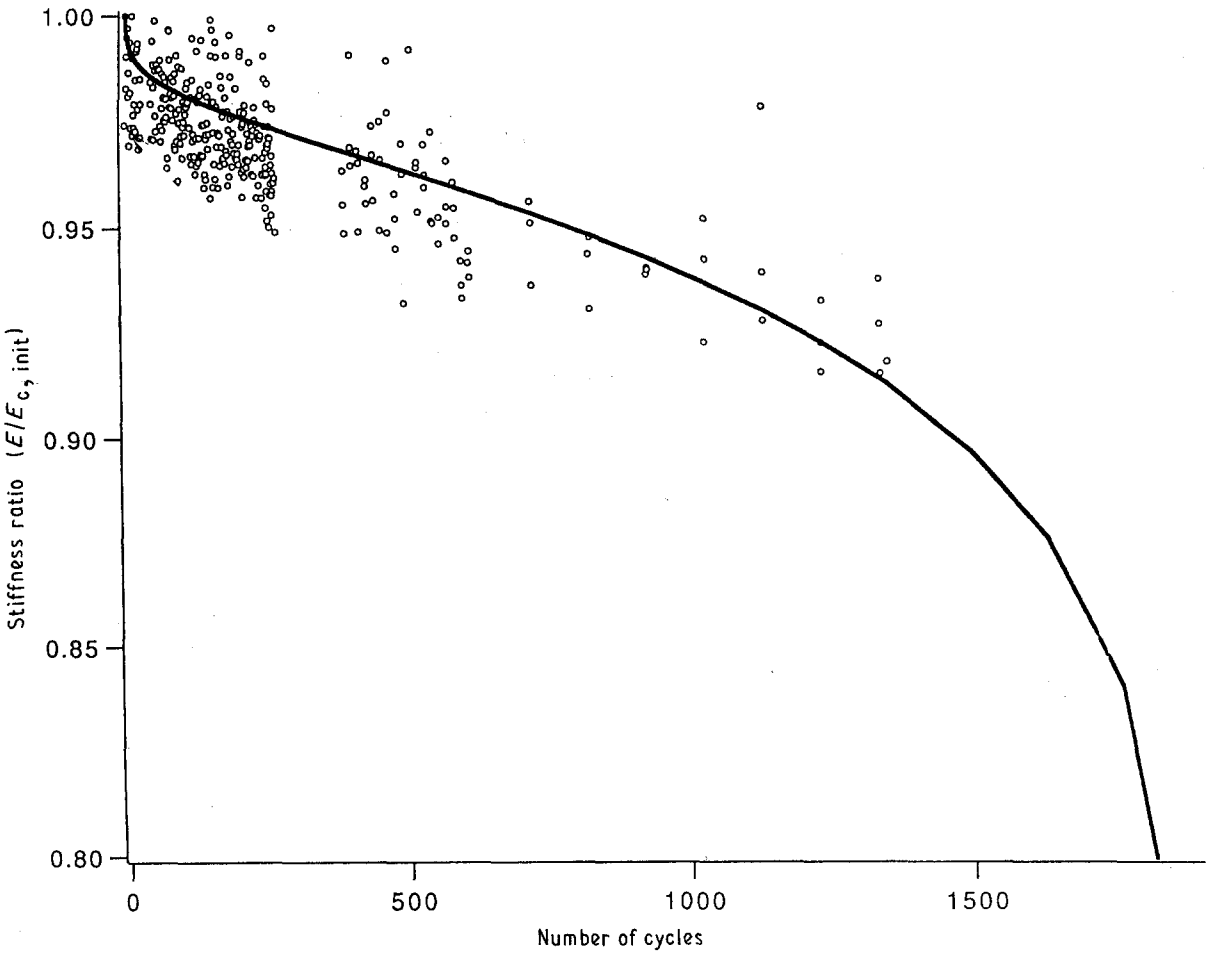

Figure 3 The predicted stiffness curve (—) for specimen 4C (Table I) with the experimental data (○) superimposed.

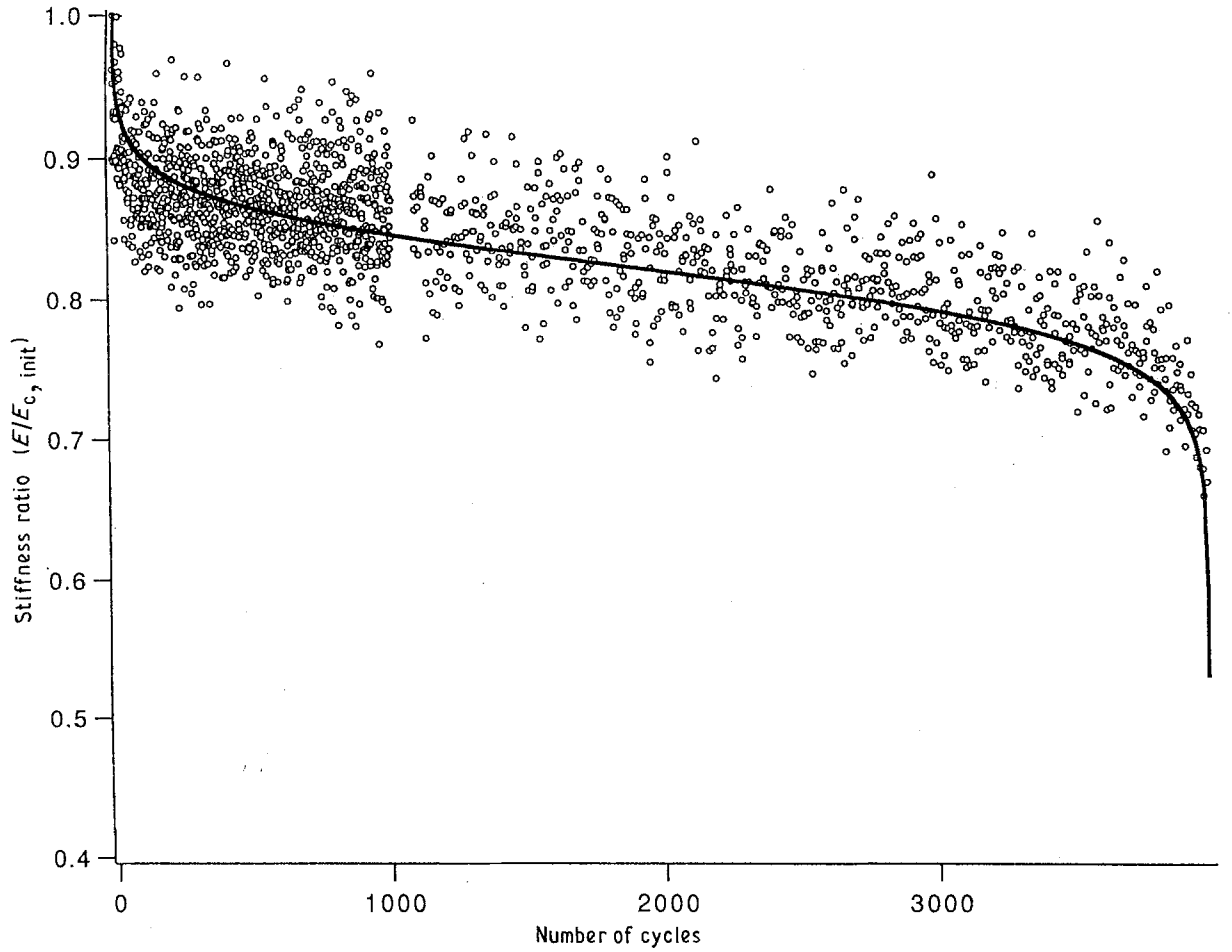

Figure 4 The predicted stiffness curve (—) for specimen 32–5 (Table I) with the experimental data (○) superimposed.

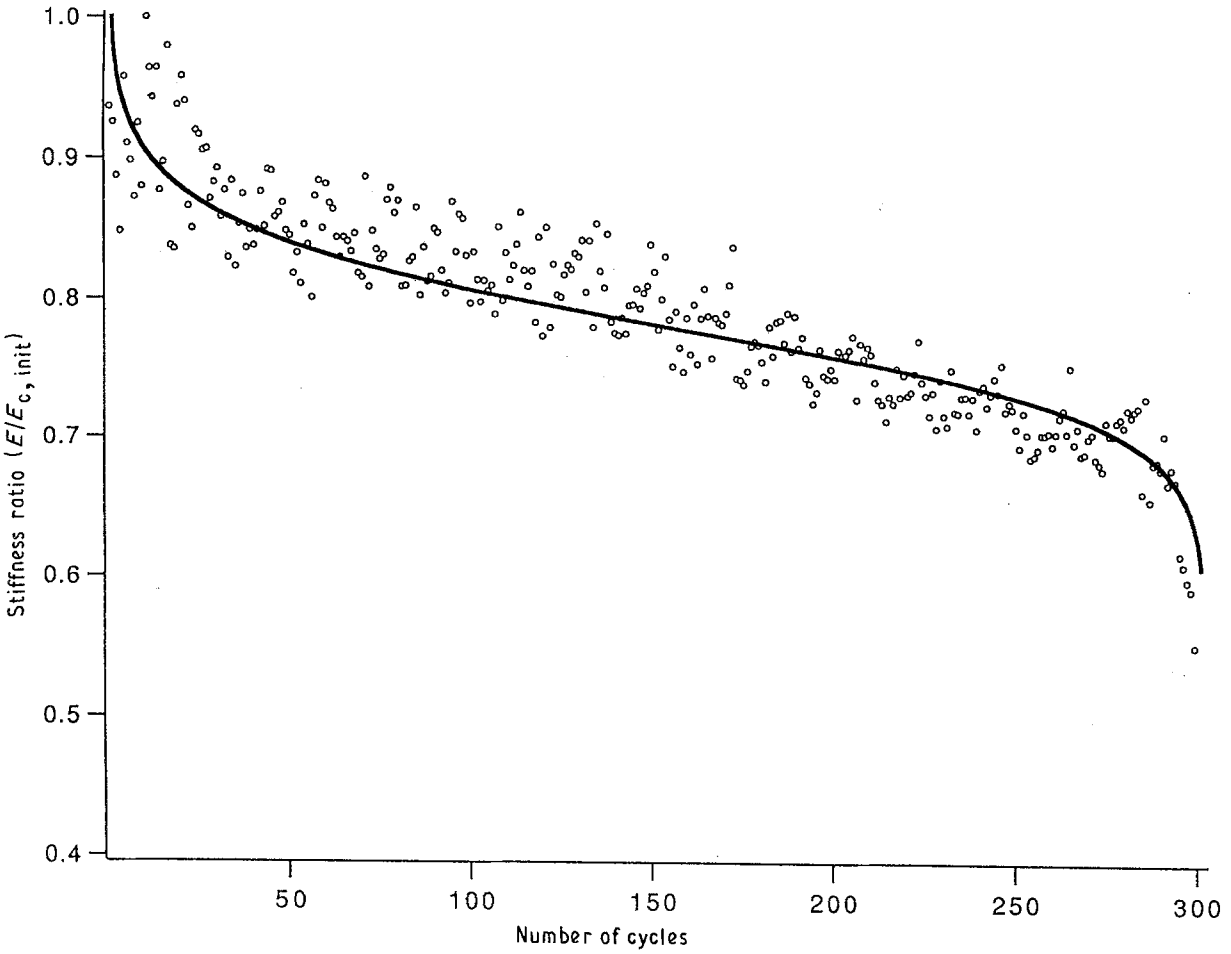

Figure 5 The predicted stiffness curve (—) for specimen 32–4 (Table I) with the experimental data (○) superimposed.

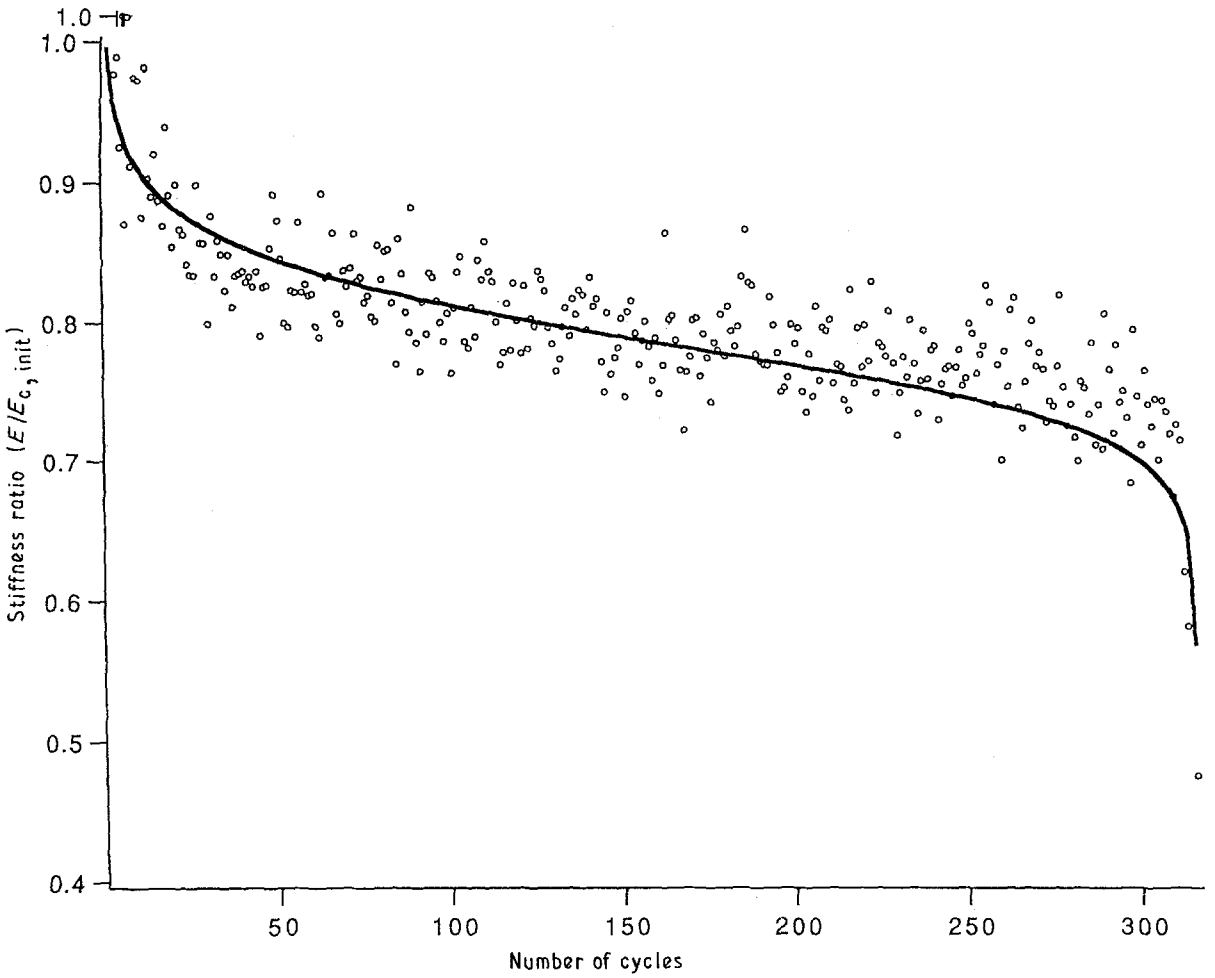

Figure 6 The predicted stiffness curve (—) for specimen 20–5 (Table I) with the experimental data (○) superimposed.

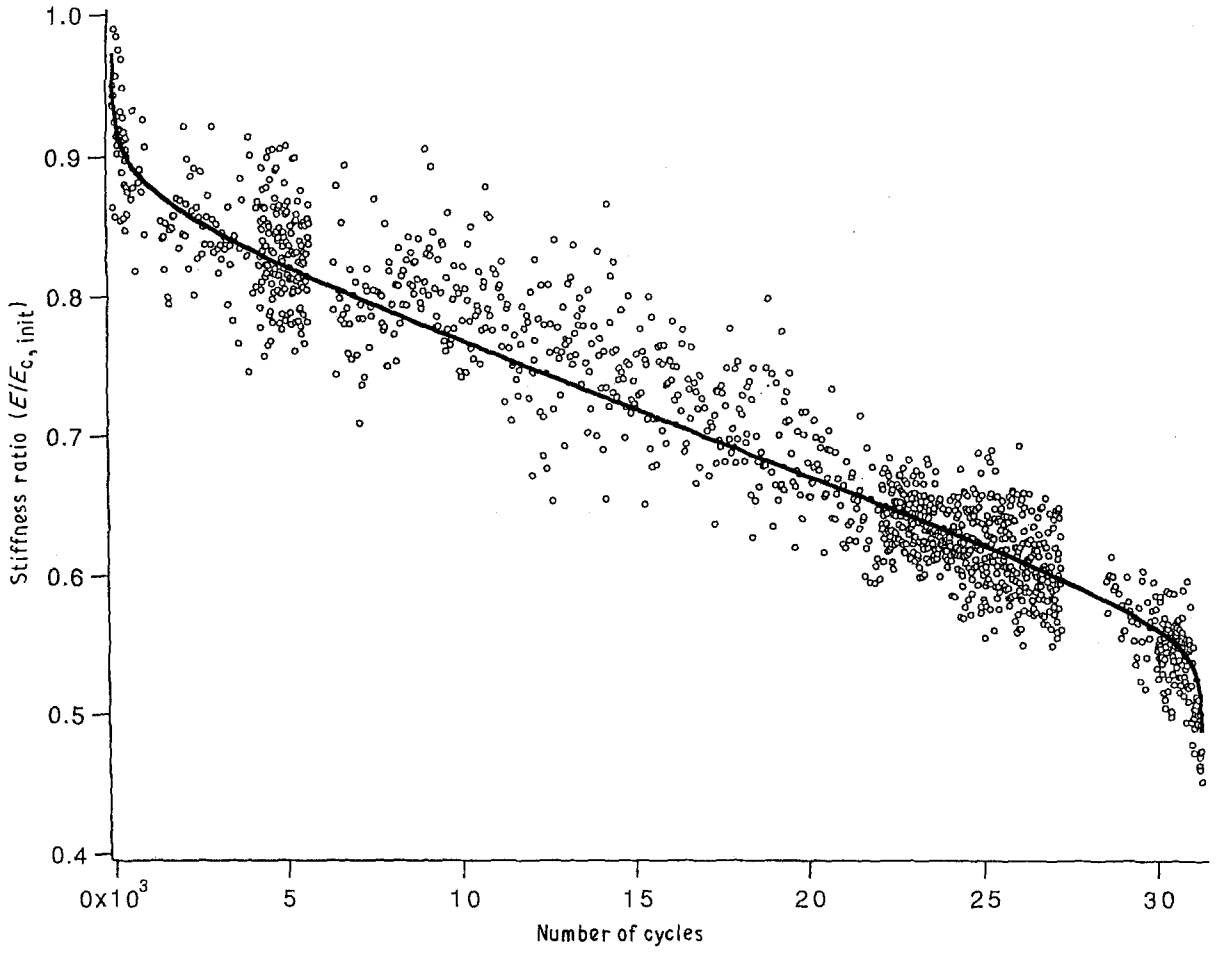

Figure 7 The predicted stiffness curve (—) for specimen 34–8 (Table I) with the experimental data (○) superimposed.

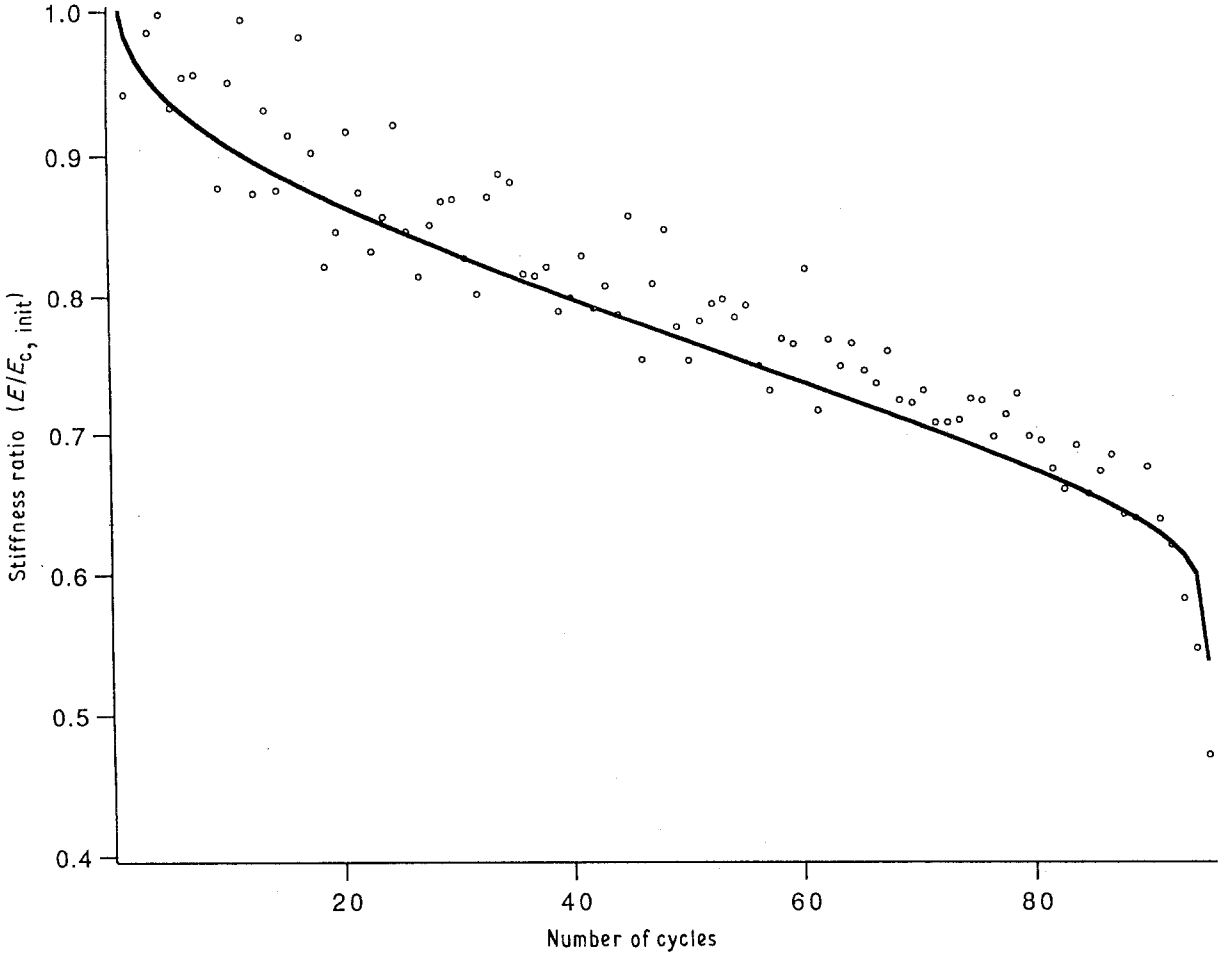

Figure 8 The predicted stiffness curve (—) for specimen 34–6 (Table I) with the experimental data (○) superimposed.

gradually continues to deteriorate; however, it is still able to support the maximum applied stress". These load–deflection traces are inserted in Fig. 9.

Talreja [6] reported the work of Butkus *et al.*, in the form of fatigue stiffness drop for various glass-ceramic matrix–Nicalon composites. In an attempt to apply the model, the stiffness versus cycles for unidirectional ($[0]_{10}$) composites consisting of Corning 1723 glass matrix and Nicalon fibres as reported in this paper [6] is compared with predictions made from the model. The following properties have been used in the prediction: $E_c = 140$ GPa (as measured from the monotonic tensile stress–strain curve) $E_f = 190$ GPa, $V_f = 0.5$, $\sigma_{uts} = 680$ MPa, $\sigma_{appl} = 500$ MPa, $N_f \simeq 200\,000$ cycles (as measured from the normalized modulus versus cycles).

The exact starting modulus of the composite and the N_f and the interface properties were not available. Therefore, E_c was assumed to be the rule-of-mixtures value and f was allowed to vary from 0 to ~ 0.5. The results of the predicted stiffness versus cycles are plotted in Fig. 10. The experimental results of Butkus *et al.*, are also presented in this figure.

In general, the agreement between the experimental and predicted stiffness is good in the early part of the life when $f = 0$ (Fig. 10). For the later part of life and other f values, the experimental data are well above the predictions. One reason for this deviation may be associated with the way the strain is measured, as mentioned in the previous section.

4. Conclusions

A mechanistically based damage-evolution model is presented to predict the stiffness changes in unidirectional brittle matrix continuous fibre-reinforced composites during fatigue. The model recognizes that the fatigue-damage evolution takes place through a sequence of events starting with the matrix cracking, followed by fibre/matrix debonding, fibre breakage and final failure. These events individually contribute to the drop in stiffness that can be calculated based on the stiffness of the matrix, fibre and the friction coefficient of the fibre/matrix interface ($f = t/s$). The stiffness changes for a borosilicate–Nicalon composite are predicted for a number of fatigue test conditions and the model is validated by experimental data. Similar comparisons between predicted versus experimental data for LAS–Nicalon and aluminosilicate–Nicalon are also presented.

Acknowledgement

The authors wish to acknowledge helpful discussions with the Wright Laboratory's Material Behavior (MLLN) group, particularly the support of Dr Ted Nicholas.

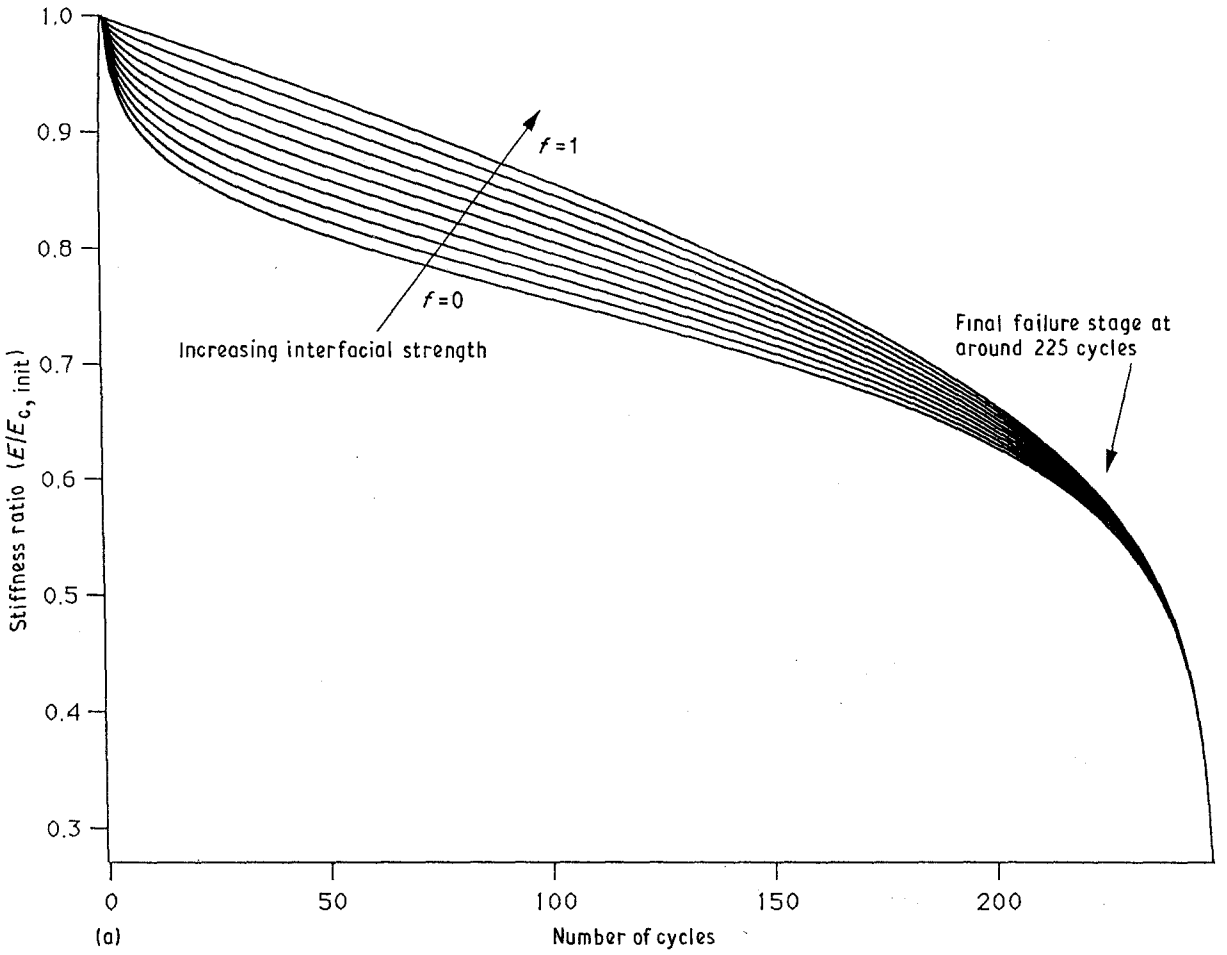

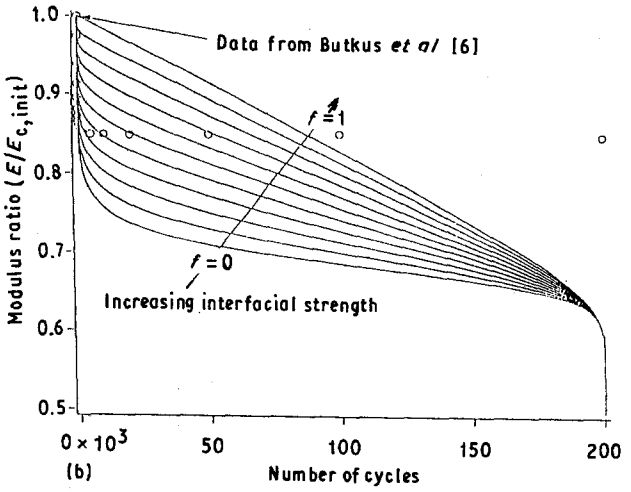

Figure 9 (a) Predicted stiffness curves for various interfacial conditions for the fatigue test [7]. (b) Load–displacement curves from the experiment for which the prediction was made [7].

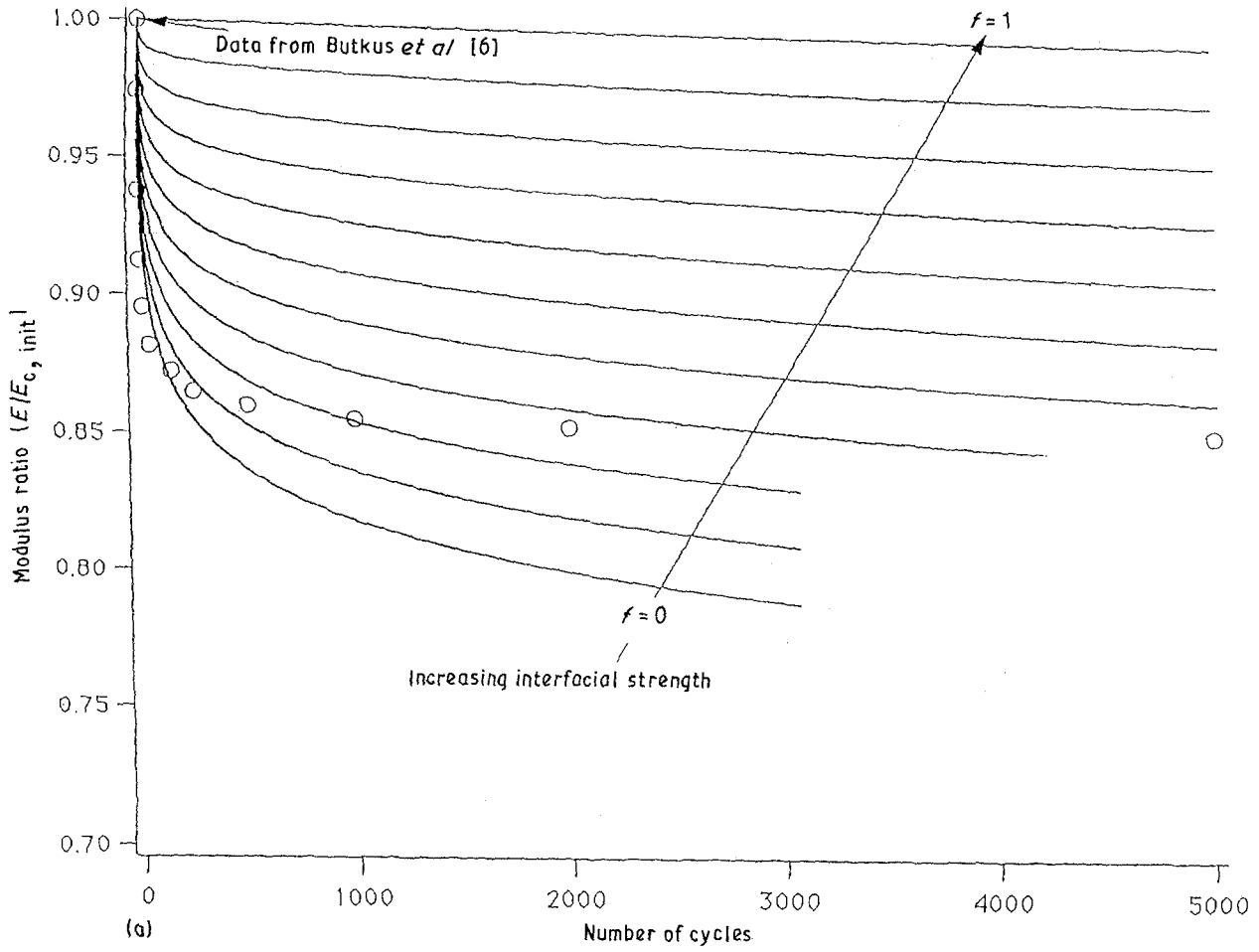

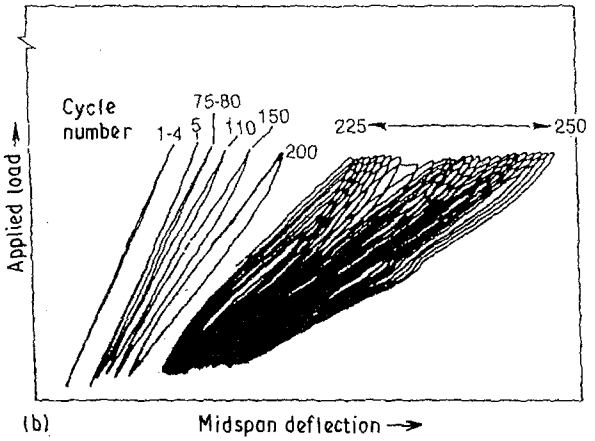

Figure 10(a) Predicted stiffness curves for various interfacial conditions for the fatigue test (1723 aluminosilicate glass) [6]. (b) Predicted stiffness curves over the entire life of the specimen [6].

References

1. K. M. PREWO, J. J. BRENNAN and G. K. LAYDEN, *Ceram. Bull.* **65** (1986) 305.
2. K. M. PREWO, *ibid.* **68** (1989) 395.
3. K. M. PREWO *et al., J. Mater. Sci.* **24** (1989) 1373.
4. K. M. PREWO and J. J. BRENNAN, *ibid.* **15** (1980) 463.
5. K. M. PREWO and E. R. THOMPSON "Research on Graphite Reinforced Glass Matrix Composites", NASA CR 165711 (1981).
6. R. TALREJA, in Proceedings of the 11th Riso International Symposium on Metallurgy and Materials Science, "Structural Ceramics – Processing, Microstructure and Properties", edited by J. J. Bentzen *et al.* (1990) pp. 145–59.
7. K. M. PREWO, *J. Mater. Sci.* **22** (1987) 2965.
8. A. POURSARTIP, M. F. ASHBY and P. W. R. BEAUMONT. *Scripta Metall.* **16** (1982) 601.
9. D. B. MARSHALL and A. G. EVANS, *J. Amer. Ceram. Soc.* **68** (5) (1985).
10. K. L. REIFSNIDER *et al.*, in "Mechanics of Composite Materials-Recent Advances", Proceedings of the IUTAM Symposium on the mechanics of Composite Materials, edited by Z. Hashin and C. T. Herakovich (Pergamon Press, New York, 1983) pp. 399–420.
11. H. C. KIM and L. J. EBERT, *J. Compos. Mater.* **12** (1978) 139.
12. RAMESH TALREJA, "Fatigue of Composite Materials" (Technomic, 1987).
13. T. K. O'BRIEN, in Damage in Composite Materials, ASTM STP-775, (American Society for Testing and Materials, Philadelphia, PA, 1982) pp. 140.
14. F. W. CROSSMAN and A. S. D. WANG, *ibid.* pp. 118.
15. W. HWANG and K. S. HAN *J. Compos. Mater.* **20** (1986) 154.
16. H. A. WHITWORTH, *ibid.* **21** (1987) 362.
17. LIN YE, *Compos. Sci. Technol.* **36** (1989) 339.
18. YANG SE-HOON, PhD thesis, George Washington University, University Microfilms Order no. DA8725939 N88-26405.
19. A. POURSARTIP, M. F. ASHBY and P. W. R. BEAUMONT, *Compos. Sci. Technol.* **25** (1986) 193.
20. *Idem, ibid.* **25** (1986) 283.
21. V. RAMAKRISHNAN and N. JAYARAMAN, *J. Mater. Sci. to be published.*
22. V. RAMAKRISHNAN and N. JAYARAMAN, to be published.
23. D. K. SHETTY, *J. Amer. Ceram. Soc.* **71** (1988) C-107.
24. J. D. BRIGHT, S. DANCHAIVIJIT and D. K. SHETTY, *ibid.* **74** (1991) 115.
25. J. J. BRENNAN, in "Tailoring of Multiphase and Composite Ceramics", edited by R. E. Tressler *et al.* Materials Science Research, Vol. 20 (Plenum, 1985) pp. 549–60.
26. R. F. COOPER and K. CHYUNG, *J. Mater. Sci.* **22** (1987) 3148.
27. E. BISCHOFF *et al., J. Amer. Ceram. Soc.* **72** (1989) 741.

Received 11 July 1991
and accepted 4 February 1992